Science Advances
AAAS

advances.sciencemag.org/cgi/content/full/5/10/eaax4295/DC1

Supplementary Materials for

What drives tectonic plates?

Nicolas Coltice*, Laurent Husson, Claudio Faccenna, Maëlis Arnould

*Corresponding author. Email: nicolas.coltice@ens.fr

Published 30 October 2019, *Sci. Adv.* **5**, eaax4295 (2019)
DOI: 10.1126/sciadv.aax4295

The PDF file includes:

Fig. S1. Close-up of relative dynamic pressure field from the cross-section shown in Fig. 2.
Fig. S2. 3D snapshots of the 10 low Ra models and the model at Earth-like convective vigor (high Rayleigh number).
Fig. S3. Initial distribution of continental material (yellow), the stiffer roots being thicker, and dense basal piles (red) in the model with high convective vigor.
Fig. S4. Properties of the mantle convection model for the snapshot of Fig. 2 and fig. S1.
Fig. S5. Temperature and viscosity profiles in the high Ra calculation.
Legends for movies S1 to S3
Table S1. Physical parameters of the reference model (low Rayleigh number) and the high Rayleigh number model.

Other Supplementary Material for this manuscript includes the following:

(available at advances.sciencemag.org/cgi/content/full/5/10/eaax4295/DC1)

Movie S1 (.avi format). Movie showing the closing of an ocean and supercontinent assembly.
Movie S2 (.avi format). Movie showing breakup sequences of a supercontinent.
Movie S3 (.avi format). Movie showing subduction initiations.

Supplementary figures

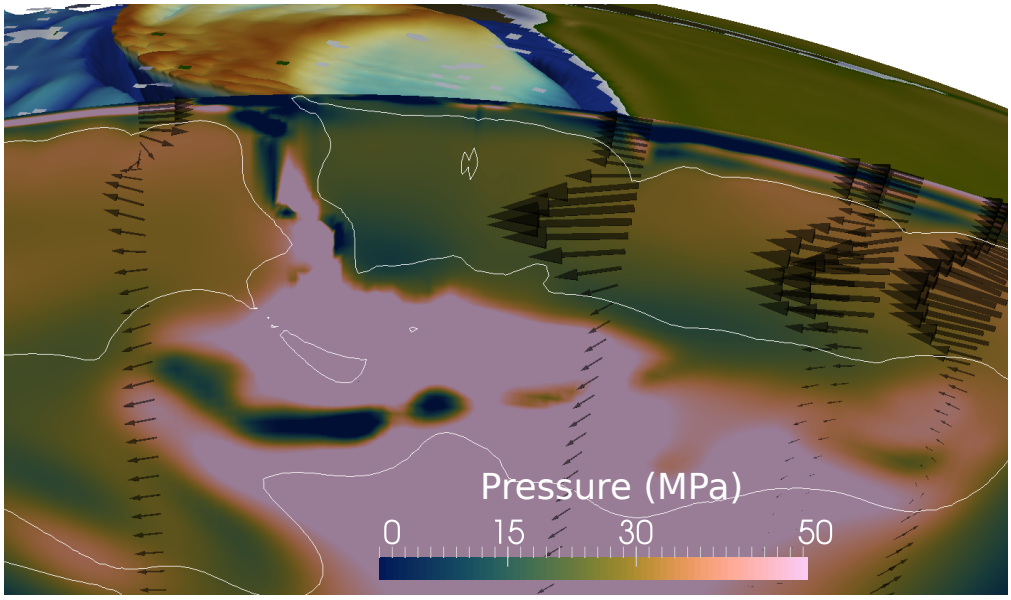

Fig. S1. Close-up of relative dynamic pressure field from the cross-section shown in Fig. 2. Black arrows represent the velocity within the plane (same scale as Fig. 2 - fastest velocities are close to 8 cm year^{-1}.) Since dynamic pressure is known in a relative way (adding a constant would not change the numerical solution of the dynamic system), we chose a value for dynamic pressure of 0 which is favorable for pressure difference estimation. The color scale of the pressure is saturated to focus on the pressure distribution within the boundary layer and just below. Dynamic pressure is very strong in the slab, because of its high viscosity. Toroidal flow around the slab is an expression of this high dynamic pressure: the softer material flows around the stiffer material. This figure shows that the subducting plate dragging the underlying mantle is driven by pressure differences in the boundary layer, i.e. trench displaying the lowest values. In the back-arc region, the interior moves faster than the surface driven by the pressure gradient below the boundary layer.

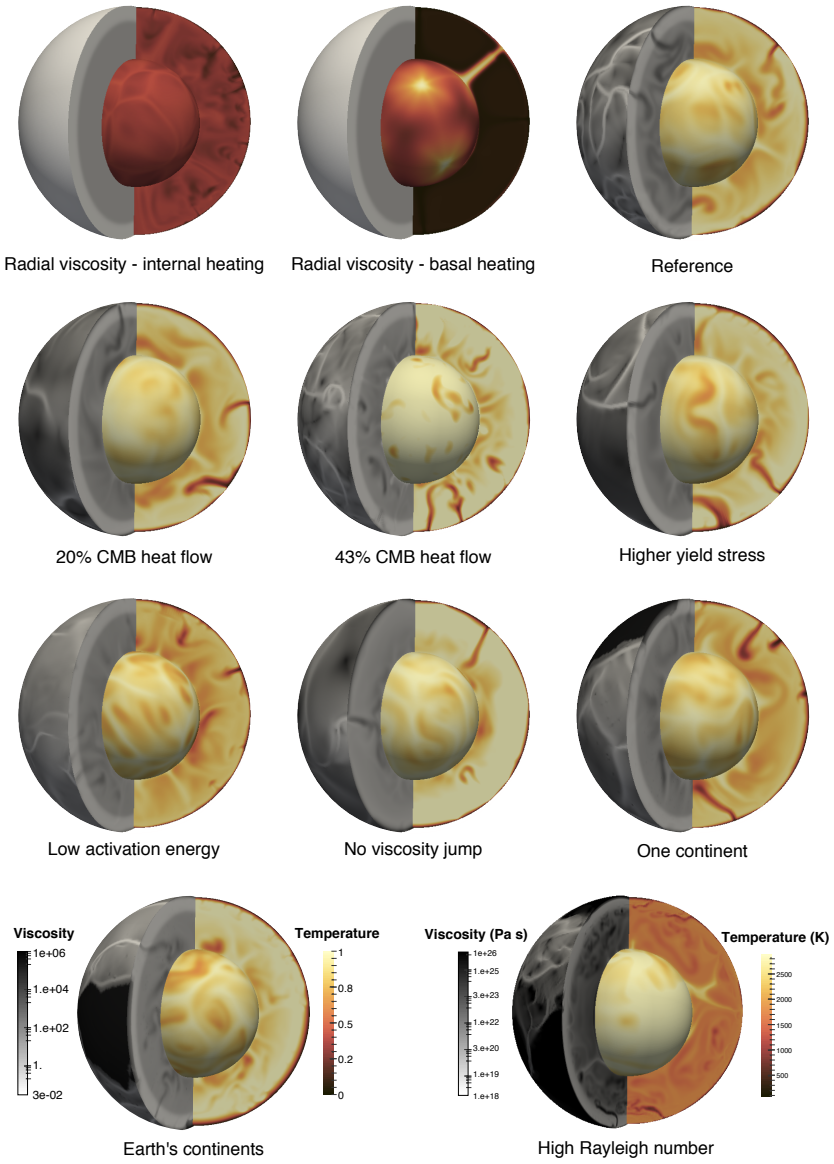

Fig. S2. 3D snapshots of the 10 low Ra models and the model at Earth-like convective vigor (high Rayleigh number). The viscosity field is represented in the left part of the shell, the temperature field shown on the right part of the shell. The temperature just above the core is mapped in the center. For the low Ra cases, viscosity and temperature are non-dimensional, the scale being represented on the snapshot of the model with Earth's continents. For the high Ra model, viscosity and temperature are dimensional.

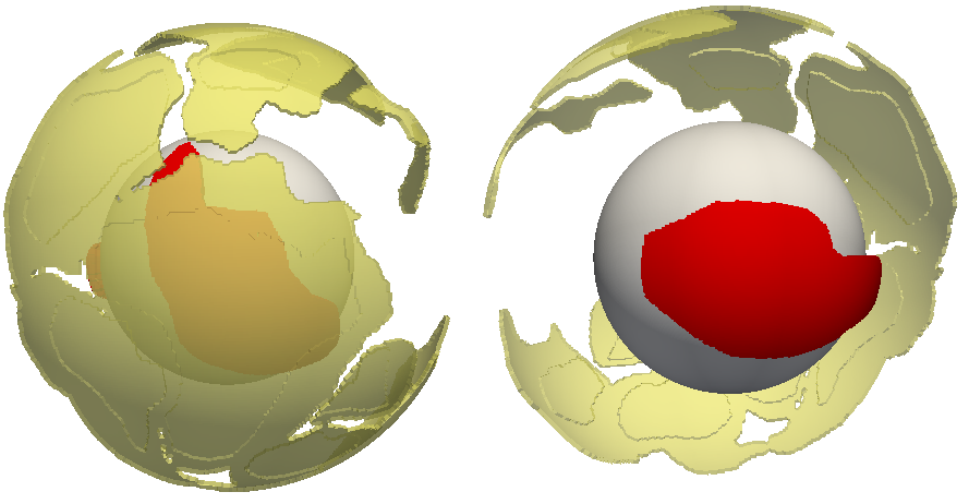

Fig. S3. Initial distribution of continental material (yellow), the stiffer roots being thicker, and dense basal piles (red) in the model with high convective vigor.

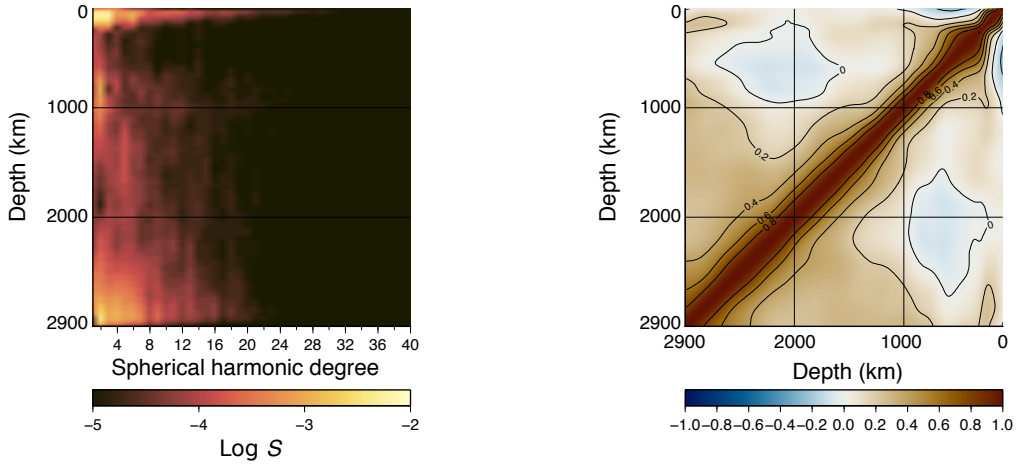

Fig. S4. Properties of the mantle convection model for the snapshot of Fig. 2 and fig. S1. (left) $LogS$, S being the normalized power spectrum of temperature heterogeneities, as a function of depth in the model. (right) Radial correlation of the temperature heterogeneities as a function of depth in the model is colored and contoured by 0.2 increment.

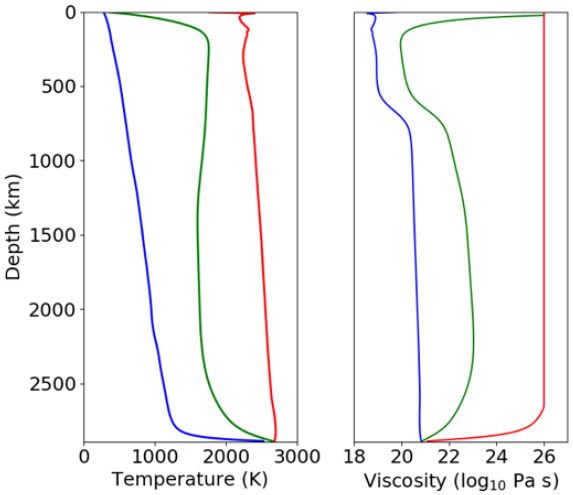

Fig. S5. Temperature and viscosity profiles in the high Ra calculation. (left) Laterally averaged temperature is shown in green. The blue profile represents minimum temperature at each depth, while the red profile represents maximum temperature. (right) Viscosity profiles in the model. Green is the viscosity profile corresponding to the average temperature profile. Blue represents the minimum viscosity and red the maximum.

Supplementary movies

Movie S1. Movie showing the closing of an ocean and supercontinent assembly. Left: the 1670 K isotherm, colored by depth from 0 to 100 km, with continents superimposed. A green shading displays strain rates larger than 10^{-16} s^{-1}. Right: translucent volumes of hot material representing ascending plumes, overprinting dark red dense basal material. This movie is 220 Ma long (10 Ma per second), between 550 and 770 Ma. Although the oceanic domain is closing, basin opening is very dynamic until continents aggregate. Dense material at the base moves very slowly and remains stable over the assembly.

Movie S2. Movie showing breakup sequences of a supercontinent. Left: the 1670 K isotherm, colored by depth from 0 to 100 km, with continents superimposed. A green shading displays strain rates larger than 10^{-16} s^{-1}. Right: translucent volumes of hot material representing ascending plumes, overprinting dark red dense basal material. This movie is 220 Ma long (10 Ma per second), between 800 and 1020 Ma. Back-arcs develops on the edges of the supercontinent, which progressively become under tension. Hotter material softens a channel where continental rifting starts, highlighted by high strain rates. A plume lies close to the initial tip of the opening. However, the first ocean opening happens in another direction, before the first failed rift is reactivated with a propagator developing from the oceanic domain.

Movie S3. Movie showing subduction initiations. Left: the 1670 K isotherm, colored by depth from 0 to 100 km, with continents superimposed. A green shading displays strain rates larger than 10^{-16} s^{-1}. Right: translucent volumes of hot material representing ascending plumes, overprinting dark red dense basal material. The 1670 K isotherm is also represented

here at depth of between 150 and 800 km, in order to visualise slab descent and subduction initiation. This movie is 100 Ma long (10 Ma per second), and starts at the same time as movie S2. It shows the initiation of two plume-induced systems close to the main latitudinal ridge and one example of ”transform” subduction initiation close to the longitudinal ridge system. It also shows fast trench retreat and slab termination wrapping in the upper mantle.

Supplementary Table

Table S1. Physical parameters of the reference model (low Rayleigh number) and the high Rayleigh number model.

Parameter	Reference (non-dimensional)	High Rayleigh number (dimensional)
Ra	10^6	10^7
Heat production rate	38	9.12×10^{-12} W kg^{-1}
T_s	0	255 K
Basal temperature	1	2645 K
T_0	N/A	1530 K
Surface thermal expansion	1	3 10^{-5} K^{-1}
Reference density	1	4000 kg.m^{-3}
Reference diffusivity	1	10^{-6} m^2 s^{-1}
Reference conductivity	1	3.15 W.m^{-1} K^{-1}
η_0	1	10^{22} Pa s
A	30	N/A
E_a	N/A	160 kJ mol^{-1}
V_a	0	13.8 cm^3 mol^{-1}
Maximum viscosity cutoff	No cutoff	10^{26} Pa s
Viscosity jump at 660 km	$\times 30$	$\times 30$
σ_Y at the surface - oceanic lithosphere	1.5 10^4	61 MPa
Yield stress gradient for all materials	0.025	1088 Pa m^{-1}
σ_Y at the surface - continental interior	N/A	122 MPa
Viscosity increase - continental interior	N/A	$\times 100$
Density deficit - continental interior	N/A	-225 kg m^{-3}
Thickness - continental interior	N/A	200 km
σ_Y at the surface - continental belt	N/A	61 MPa
Viscosity increase - continental belt	N/A	$\times 50$
Buoyancy number - continental belt	N/A	-225 kg m^{-3}
Thickness - continental belt	N/A	125 km
σ_Y at the surface - weak layer	N/A	10 MPa
Viscosity drop - weak layer	N/A	$\times 0.1$
Thickness - weak layer	N/A	14 km
Viscosity increase - LLSVPs	N/A	$\times 10$
Density excess - LLSVPs	N/A	137 kg m^{-3}
Initial thickness - LLSVPs	N/A	500 km